2011

Mechanical response of pig skin under dynamic tensile loading

Jaeyoung Lim
Purdue University

Jihye Hong
Purdue University

Weinong W. Chen
Purdue University, wchen@purdue.edu

Tusit Weerasooriya
US Army Research Laboratory

International Journal of Impact Engineering 38 (2011) 130–135

Contents lists available at ScienceDirect

International Journal of Impact Engineering

journal homepage: www.elsevier.com/locate/ijimpeng

Mechanical response of pig skin under dynamic tensile loading

Jaeyoung Lim [a], Jihye Hong [a], Weinong W. Chen [a,*], Tusit Weerasooriya [b]

[a] Schools of Aeronautics/Astronautics and Materials Engineering, Purdue University, West Lafayette, IN 47907, United States
[b] US Army Research Laboratory, Aberdeen Proving Ground, MD 20005, United States

A R T I C L E I N F O

Article history:
Received 8 March 2010
Received in revised form
30 August 2010
Accepted 15 September 2010
Available online 22 September 2010

Keywords:
Kolsky bar
SHTB
Dynamic tension
Mechanical response
Porcine skin

A B S T R A C T

Uniaxial tensile experiments were performed on pig skin to investigate the tensile stress–strain response at both quasi-static and dynamic rates of deformation. A Kolsky tension bar, also called a split Hopkinson tension bar (SHTB), was modified to conduct the dynamic experiments. Semiconductor strain gages were used to measure the low levels of the transmitted signal from pig skin. A pulse shaper technique was used for generating a suitable incident pulse to ensure stress equilibrium and approximate constant strain rate in the specimen of a thin skin sheet wrapped around the ends of the bars for minimizing radial inertia. In order to investigate the strain-rate effect over a wide range of strain rates, quasi-static tests were also performed. The experimental results show that pig skin exhibits rate-sensitive, orthotropic, and non-linear behavior. The response along the spine direction is stiffer at lower rate but is less rate sensitive than the perpendicular direction. An Ogden model with two material constants is adopted to describe the rate-sensitive tensile behavior of the pig skin.

1. Introduction

The mechanical behavior of biological tissues under dynamic loading has been an interest in various applications, ranging from mechanical modeling of the body parts for the surgical reconstruction procedures using the body tissues to the prediction of human skin damage caused by vehicle crashes or punching accidents [1–3]. In order to understand the rate-dependent mechanical response of biological tissues during impact accidents, it is essential to know the proper constitutive model of biological tissues with corresponding material constants determined experimentally from quasi-static to high loading rates. However, most of the studies on biological tissues in literature have been focused on the low strain-rate response. This is primarily due to the experimental difficulties associated with dynamic testing of materials, especially on soft materials [4]. Therefore, few experimental results on biological tissues under high-rate loading are available. Song et al. [5] showed that the compressive stress–strain response of porcine muscle is highly strain-rate sensitive. Pervin and Chen [6] performed dynamic compressive experiments on brain tissues at various strain rates. Cheng et al. [7] conducted high-rate tensile experiments on bovine tendon and observed dynamic Mullins effects on its stress–stretch behavior.

Pig skin is one of the substitute materials for studying human skin due to its similarity in material response to human skin [8,9]. Skin has a layered structure with its stiffness controlled by the arrangement and density of the collagen and elastin fibers [10,11]. Since the collagen fibers have a preferred orientation, skin is typically considered to be an inhomogeneous, orthotropic, and rate-dependent material [2,9]. Shergold et al. recently show an orthotropic behavior and strain-rate sensitivity of pig skin in uniaxial compression tests at both quasi-static and high rates. However, no experimental results on biological skin under high-rate tensile loading are available despite the fact that many failures are tensile in nature. Due to the nature of the skin material, it is expected that its tensile mechanical response is highly rate dependent. Quasi-static material response may not be extrapolated to the high-rate range without experimental validation.

In this article, a modified split Hopkinson tension bar (SHTB), also known as a Kolsky tension bar, was used to determine the tensile behavior of pig skin at high strain rates. Semiconductor strain gages were used to measure the low transmitted signals. Controlled incident pulses ensure that the specimen deforms under dynamic stress equilibrium at constant strain rates. An Ogden model was used to fit the experimental results.

2. Materials and specimens

Fresh pig skin was obtained from a local butcher shop immediately after slaughtering. The animal was a large crossbred white pig, 9 months old, with a weight of about 135 kg. The skin was preserved in 0.9% normal saline solution with a temperature of

* Corresponding author. Tel.: +1 765 494 1788; fax: +1 765 494 0307.
E-mail address: wchen@purdue.edu (W.W. Chen).

0734-743X/$ – see front matter © 2010 Elsevier Ltd. All rights reserved.
doi:10.1016/j.ijimpeng.2010.09.003

4 °C. The abdominal area of the pig skin was cut to make specimens as shown in Fig. 1. All of the fat layer, the outer epidermis, and hairs were carefully removed from the specimens using a surgical scalpel.

The specimens from the dermis were 40-mm long, 25-mm wide and 2-mm thick. They were divided into two groups with respect to the testing directions and are indicated in Fig. 1(a): One group of samples was cut with the length direction along the direction of pig spine. The other group was prepared with length perpendicular to the direction of pig spine. The samples were mounted in a tubular shape completely enclosed around the bar ends. This thin-wall tubular geometry minimizes the radial inertia effects on measurements [12]. The non-uniformity of the specimens shown in Fig. 1 is mainly in the plane directions of the skin. The skin specimen is actually wrapped around the test section of a fixed length. The more important dimension is thus the thickness, the average value of which was individually measured from four different locations. A short gage length of 2 mm is necessary to facilitate dynamic equilibrium across the length of the soft specimen. Longer specimen is preferred to minimize end effects. However such geometries are not feasible at the strain rates we intended to conduct experiments. To allow the specimen to be loaded uniformly, the end effects on the high-rate response of biological tissues are a by-product and will have to be further studied in the future.

3. Static and dynamic experimental setup

An MTS 810 testing machine was used to perform the quasi-static tensile experiments. Tensile load and displacement were measured directly by a load cell with a capacity of 220.24 N (50 lbf) and an extensometer of ±1.25 mm, respectively. Fig. 2 also shows the configuration of the grip system for pig skin tubular specimens.

Two grip strips, which are thin metal strips with rough gripping surfaces, attached to both the bar surface and the inner surface of the clamp. A skin sheet then wrap the grip strips around the two ends of the bars to form tubular shape of the specimen. Plastic clamps are used to press the skin specimen to the bar ends.

To investigate the tensile behavior of pig skin at high rates, we modified a Kolsky tension bar [13], also called a split Hopkinson tension Bar (SHTB). SHTB has been widely used to determine dynamic tensile behavior of materials at high strain rates [14,15]. To conduct tensile experiments on soft tissues, further modifications are necessary to ensure valid testing conditions on the specimen. Fig. 3 shows the experimental setup of a modified Kolsky tension bar used in this study. The modified system consists of a momentum bar, a striker tube, a compound incident bar, and a transmission bar. The incident bar is composed of a high strength maraging steel rod and an aluminum alloy rod with a diameter of 19 mm, 12.7 mm and a length of 2286 mm, 1830 mm, respectively. The transmission bar is made of an aluminum alloy rod with a diameter of 12.7 mm and a length of 1830 mm. The impact tube of steel with a length of 533 mm is free to slide on the outer surface of the steel incident bar. As the striker tube, driven by pressurized air in a gas gun, impacts the flange head of the steel incident bar, a tensile stress wave is generated and propagates through the incident bar. As the tensile stress wave reaches the joint between the steel portion and the aluminum portion of the incident bar, part of the wave is reflected back into the steel incident bar because the impedance mismatches between the steel and aluminum incident bars, and the rest continues to propagate in the aluminum incident bar to the specimen. This compound incident bar is necessary to allow consistent impact conditions while not overloading the soft skin specimen. When the incident pulse arrives at the specimen, the elastic pulse is partly reflected back to the incident bar and partly transmitted through the specimen. In the experimental setup used in this study, the transmitted strain signal is recorded from the semiconductor strain gages, which are glued to the transmission bar and used to measure weak signals associated with soft tissue specimens.

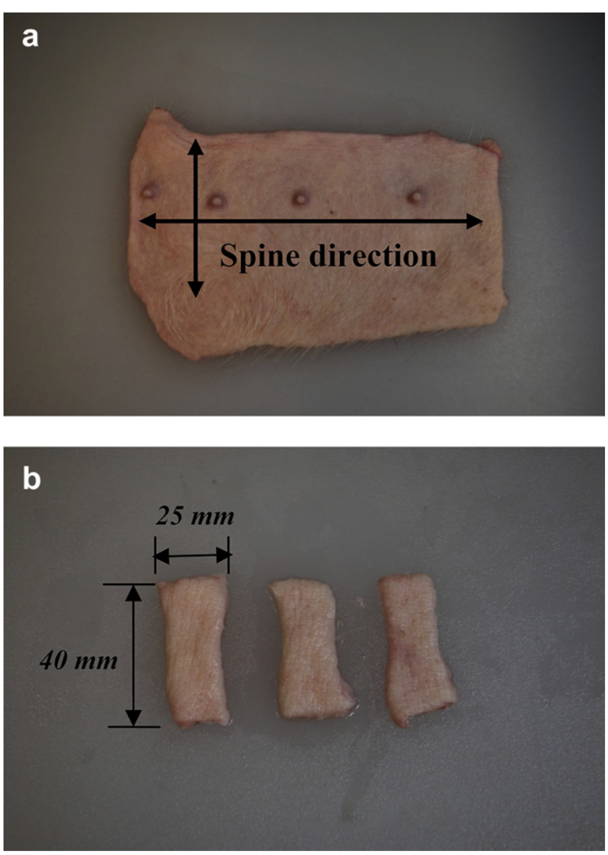

Fig. 1. Photographs of the pig skin specimens. (a) Abdominal region indicating two orthogonal directions. (b) Geometry of 2-mm thick pig skin specimens.

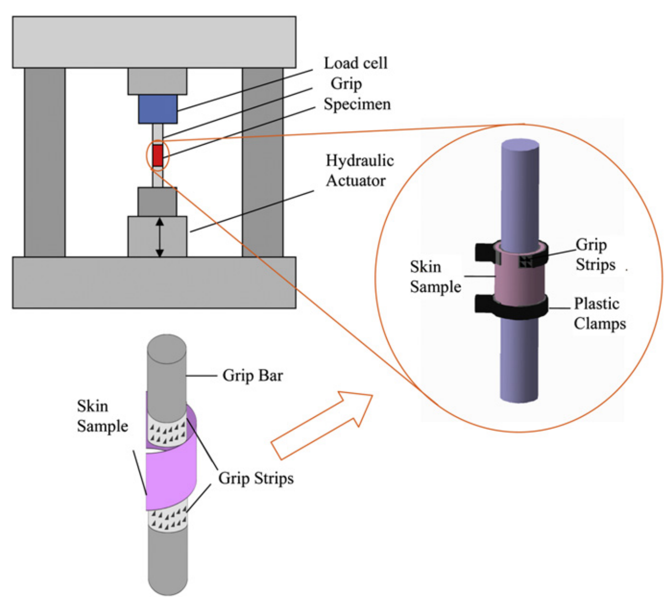

Fig. 2. Quasi-static uniaxial tension experimental setup.

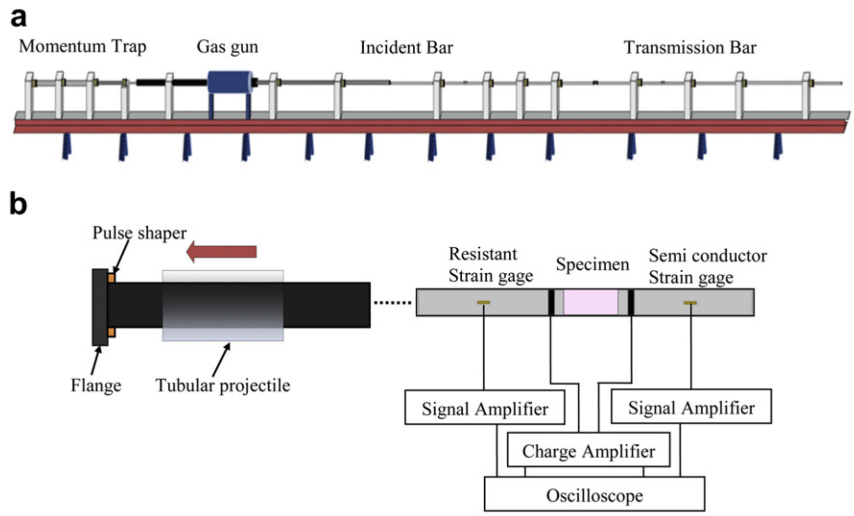

Fig. 3. The experimental setup of a modified Kolsky tension bar: (a) Illustration of the system. (b) Schematic diagram.

The striker needs to move above a minimum speed to obtain consistent repeatable velocities. Incident pulses that are generated from velocities above this minimum are too high for soft tissue experiments. To generate low-amplitude incident pulses, while allowing the striker move at above minimum speed, a combination of the momentum diversion bar and the compound incident bar was employed in this system. By absorbing most of the impact energy of the striker in the momentum diversion bar and by reducing the impedance in the incident bar between its steel portion and aluminum portion, a repeatable low-amplitude incident pulse was generated at higher striker impact velocities [16].

Fig. 4 shows the configuration of the gripping system for pig skin experiments at high strain rates. The clamped thin-tubular specimen geometry shown in Fig. 4 is adopted to minimize radial inertia effect [12,16]. Tubular shape specimen with a short gage length of 2 mm is connected to the ends of the incident and transmission bars with clamps. As shown in Fig. 4, the inner surfaces of the clamps and outer surfaces of the ends of the bars are enclosed by the grip strips, which have rough clamping surfaces to minimize the shear deformation within the gripped area and to prevent any slippage from the grips.

The time histories of the incident, reflected, and transmitted strain signals obtained from such a dynamic experiment are shown in Fig. 5(a). The strain signals on the incident and the transmission bar are recorded through strain gages mounted on these bars. A

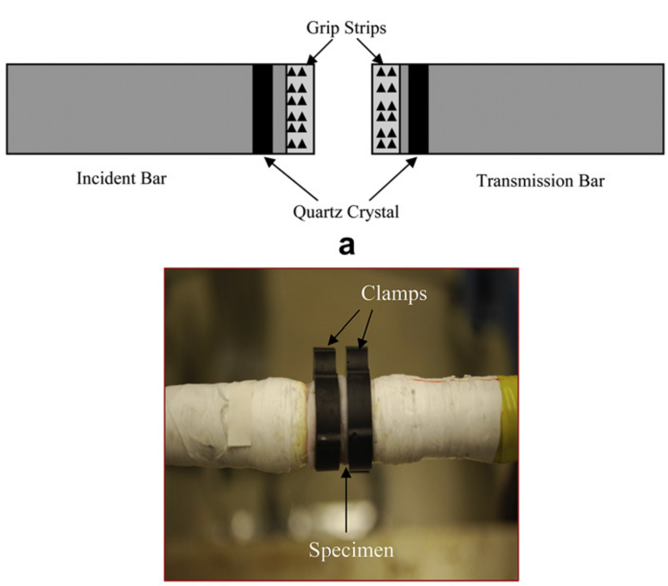

Fig. 4. Attached tubular specimen, (a) illustrating the gripping method and (b) showing the skin tissue sample mounted on the bar.

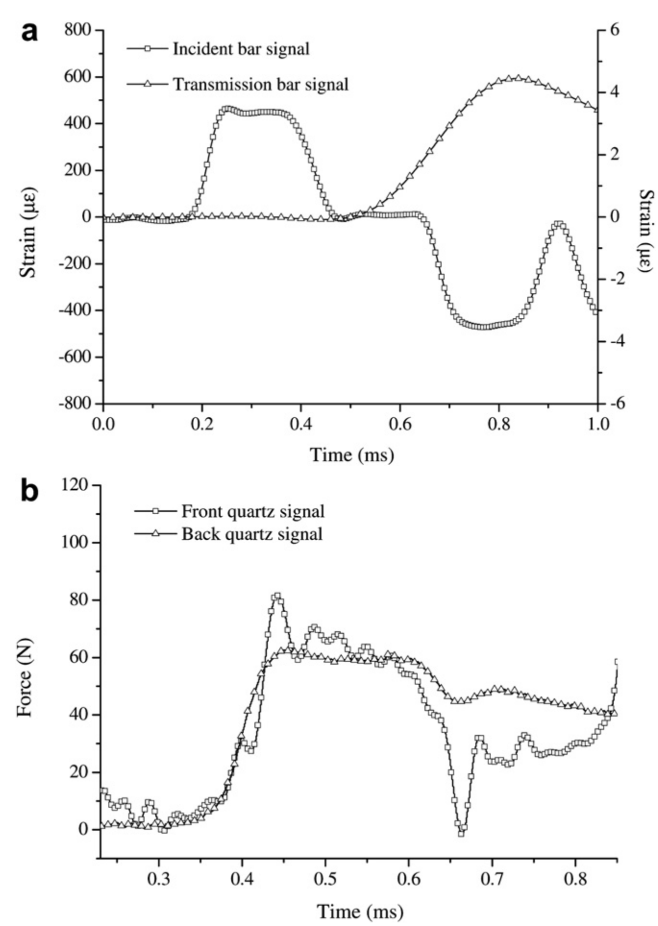

Fig. 5. Typical signals recorded from a modified Kolsky tension bar experiment on pig skin at a strain rate of $\dot{\varepsilon} \approx 2500\ s^{-1}$; (a) incident, reflected, and transmitted strain histories (b) quartz force histories.

pulse shaper [17,18] of a copper alloy 110 with a thickness of 0.05 mm was used to obtain a suitable incident pulse, which ensures the dynamic stress equilibrium at a nearly constant strain rate. Fig. 5(b) shows the force histories measured from the quartz force transducers installed on both ends of the skin specimen, indicating dynamic equilibrium in the specimen [19,20]. Since the specimen is in force equilibrium, the strain rate ($\dot{\varepsilon}$) in the specimen is calculated using the following equation:

$$\dot{\varepsilon}(t) = -\frac{2c_0}{l_s}\varepsilon_r(t) \quad (1)$$

where l_s is the initial gage length of the specimen, c_0 is the elastic bar wave speed in the rod, and ε_r is the reflected strain, respectively. By integration, we obtain the strain in the specimen as a function of time t. The stress (σ_s) in the specimen is obtained by measuring the transmitted wave (ε_t):

$$\sigma_s(t) = \frac{A_t}{A_s}E_t\varepsilon_t(t) \quad (2)$$

where E_t is Young's modulus of the bar, ε_t is the transmitted strain, A_t and A_s are the cross-sectional areas of the bar and specimen, respectively.

4. Experimental results and strain-rate effects

The quasi-static tensile experiments were performed at two strain rates by controlling the displacement rate on the hydraulic load frame. Fig. 6 shows the tensile stress–strain behavior of pig skin in terms of the engineering stress and strain at strain rates of 0.005/s and 0.5/s, with the loading direction in parallel and perpendicular to the pig spine. Each of the curves shown in Fig. 6 is the average of three repeated experiments on three specimens conducted under identical conditions. The curves show that the stress–strain response of the pig skin is non-linear with a J-shape. As shown in Fig. 6, the tensile response of pig skin demonstrates a clear distinction in its two orthogonal directions, which is consistent with the results reported in previous work [2]. Our stress–strain data on pig skin at a strain rate of 0.005/s are very close to the data on human skin obtained by Dunn et al. [21], which are also plotted for comparison in Fig. 6. The tensile test data on human skin by Dunn et al. are used to develop the constitutive model of skin in literature [10,11]. However, the stress–strain data obtained in this study are significantly different from those obtained from tensile test on human abdominal skin by Jansen and Rottier [22]. Shergold et al. [9] fitted tensile test data from Jansen and Rottier using one term Ogden model. It is clear that the stress–strain response on skin may vary widely; some of the reasons for these observed variations may be due to sample variations and variability in testing conditions such as gripping conditions.

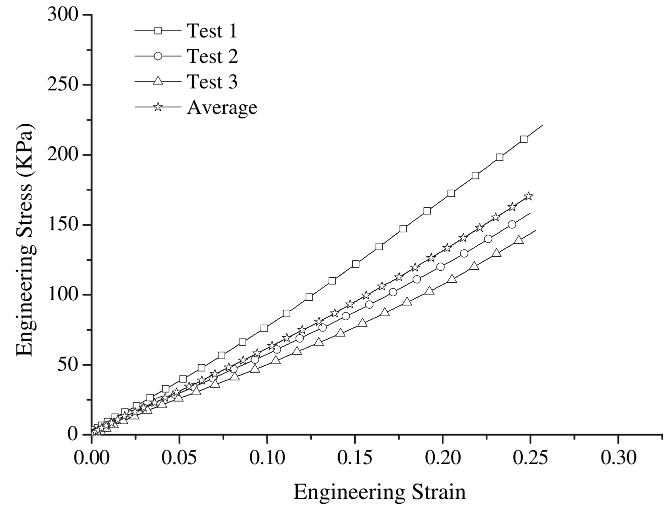

Fig. 7. Tensile stress–strain curves from three repeated tests on pig skin perpendicular to the direction of pig spine at a strain rate of 2500/s.

In addition to quasi-static testing, the pulse-shaped SHTB was used to perform high strain-rate tensile experiments on pig skin. As shown in Fig 5, the incident pulse with a constant-amplitude is achieved using a pulse shaper, which produces a nearly constant strain-rate deformation during the experiment as indicated by the reflected signal in Fig. 5. In order to examine the rate effects on the tensile behavior of pig skin, tensile experiments were performed at three high strain rates of 1700, 2500, and 3500/s. As in the slower rate experiments, three repeated experiments on three fresh specimens were conducted for each strain rate under identical testing conditions. The average thickness of each specimen, which was individually measured at four different locations, was about 1.90 mm. Fig. 7 shows the average curve of these tests at 2500/s

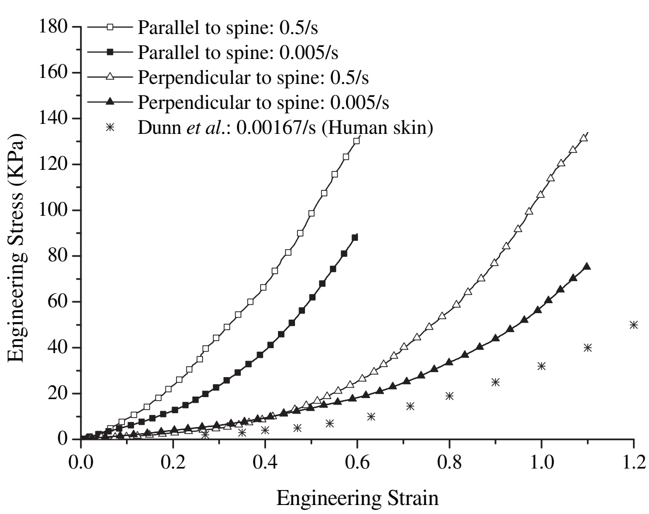

Fig. 6. Tensile stress–strain curves of pig skin at strain rates of 0.5 and 0.005/s. The data for human skin by Dunn et al. are also plotted for comparison.

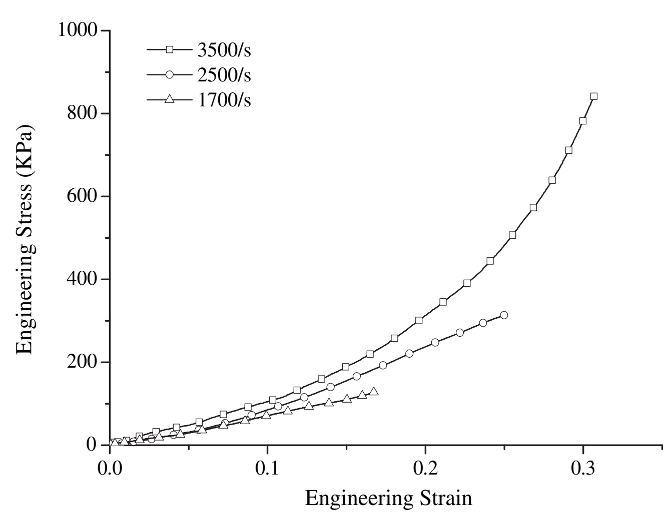

Fig. 8. Tensile stress–strain curves on pig skin along the direction of pig spine at various strain rates.

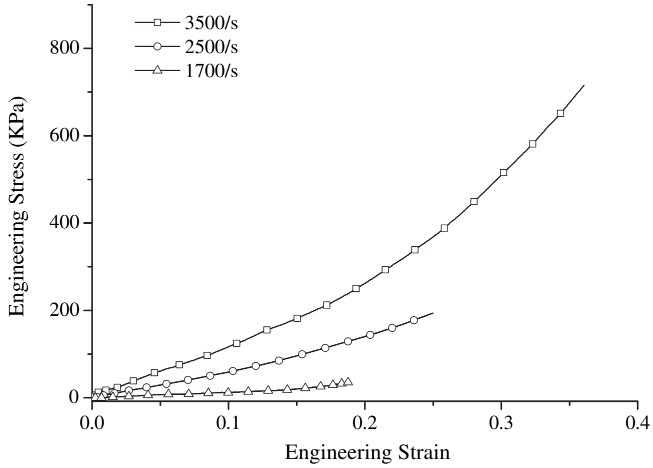

Fig. 9. Tensile stress–strain curves on pig skin perpendicular to the direction of pig spine at various strain rates.

strain rate, in addition to the stress–strain curves from three repeated experiments, which demonstrate the reasonable scatter associated with the tensile tests on pig skin tissues.

Figs. 8 and 9 show the average tensile stress–strain behavior of pig skin at high strain rates along two orthogonal directions. The strain-rate effects are clearly observed in the stress–strain response. As shown in Figs. 8 and 9, the strain-rate dependency perpendicular to the direction of pig spine is more sensitive than that along the direction of pig spine.

5. Constitutive model

In order to describe the non-linear tensile stress–strain behavior of pig skin, we used the Ogden material model. The Ogden model, first developed by Ogden [23] in 1972, has been widely used to determine the stress–strain relations of hyper-elastic materials such as rubbers, polymers, and biological tissue. In the Ogden model, the materials can be generally regarded as isotropic, incompressible, and hyper-elastic. By introducing the strain energy function, the stress–strain relations of materials can be derived. In one term Odgen model, the strain energy function denoted as W can be expressed in terms of principal stretches λ_i in Cartesian coordinate system (x_1, x_2, x_3) as follows:

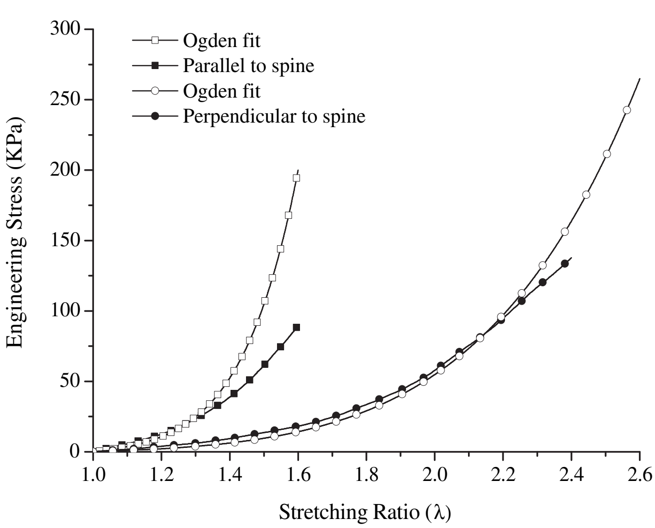

Fig. 10. The engineering stress versus stretch ratio response of pig skin at a strain rate of 0.005/s.

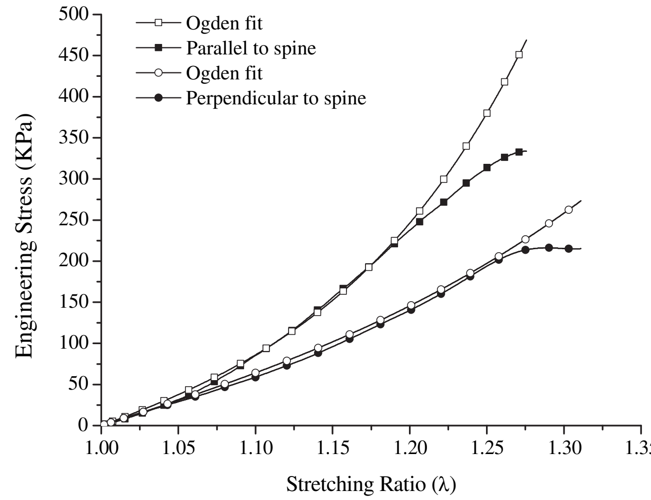

Fig. 11. The engineering stress versus stretch ratio response of pig skin at a strain rate of 2500/s.

$$W(\lambda_1, \lambda_2, \lambda_3) = \frac{2\mu}{\alpha^2}\left(\lambda_1^\alpha + \lambda_2^\alpha + \lambda_3^\alpha - 3\right) \quad (3)$$

where μ and α material constants are the shear modulus and strain hardening exponent, respectively. For an incompressible material, the principal stretches satisfy the constraint as:

$$\lambda_1\lambda_2\lambda_3 = 1 \quad (4)$$

The strain energy function can be expressed as a function of two independent stretches using Eqs. (3) and (4):

$$\widehat{W}(\lambda_1, \lambda_2) = W\left(\lambda_1, \lambda_2, \lambda_1^{-1}\lambda_2^{-1}\right) = \frac{2\mu}{\alpha^2}\left(\lambda_1^\alpha + \lambda_2^\alpha + \lambda_1^{-\alpha}\lambda_2^{-\alpha} - 3\right) \quad (5)$$

In a plane stress condition $\sigma_3 = 0$, the nominal stresses σ_i are given by [24]:

$$\sigma_1 = \frac{\partial \widehat{W}}{\partial \lambda_1}, \quad \sigma_2 = \frac{\partial \widehat{W}}{\partial \lambda_2} \quad (6)$$

For a uniaxial tension test with the loading direction along the x_1 axis, the nominal stresses can be written as follows:

$$\sigma_1 = \frac{2\mu}{\alpha}\left[\lambda^{\alpha-1} - \lambda^{-1-(\alpha/2)}\right], \quad \sigma_2 = 0 \quad (7)$$

Two constants used in the Ogden model can be determined by experiments. Figs. 10 and 11 represent the tensile stress–strain curves fitted with the one term Ogden model at quasi-static and high strain rate. The Ogden constants determined experimentally at different strain rates are summarized in Table 1. The Ogden, even with only one term, provided a good approximation to the experimental data as shown in Figs. 10 and 11, respectively.

Table 1
Material constants (μ and α) obtained at different strain rates for Ogden constitutive model of pig skin.

Strain rate (/s)	Shear modulus, μ (kPa)	Strain hardening exponent, α
0.005	10 / 3	11 / 7
0.5	20 / 8	11 / 7
1700	180 / 40	11 / 7
2500	230 / 200	11 / 7
3500	300 / 370	11 / 7

* / * indicate the parallel and perpendicular direction to the spine in pig sample.

6. Conclusions

The tensile stress–strain response of pig skin was investigated under uniaxial stress loading conditions at both quasi-static and dynamic strain rates. A modified Kolsky tension bar was used to conduct the high strain-rate experiments along the two orthotropic directions of the pig skin. Two high-resistance semiconductor strain gages on the transmission bar were used to measure the low transmitted signal. The loading pulse profile was controlled such that the skin specimen deforms at a constant strain rate under uniform loading. A thin-walled tubular shape specimen is used to minimize the radial inertia effect on the deforming specimen at high strain rate. The quasi-static tensile experiments were also performed at two strain rates under displacement control condition to examine the strain-rate effects over a wider range. Experimental results show that pig skin exhibits distinct orthotropic material behavior with respect to the spine direction of pig skin. Strain-rate dependency perpendicular to the direction of pig spine is more sensitive than that along the direction of pig spine. The strain-rate effects on the non-linear stress–strain behavior are apparent as observed from experiments at different strain rates. An Ogden model with one term is sufficient to represent the tensile response of pig skin at each strain rate. Two constants are needed for a good approximation to the experimental data over a wide range of strain rates.

References

[1] King AI. Fundamentals of impact biomechanics: Part I—biomechanics of the head, neck, and thorax. Annu Rev Biomed Eng 2000;2:55–81.
[2] Ankerson J, Birkbeck AE, Thomson RD, Vanezis P. Puncture resistance and tensile strength of skin stimulants. Proc Inst Mech Eng 1999;213(Part H): 493–501.
[3] Shergold OA, Fleck NA. Experimental investigation into the deep penetration of soft solids by sharp and blunt punches, with application to the piercing of skin. J Biomech Eng 2005;127:838–48.
[4] Song B, Chen W. Split Hopkinson bar techniques for characterizing soft materials. Lat Am J Solid Struct 2005;2:113–52.
[5] Song B, Ge Y, Chen W, Weerasooriya T. Dynamic and quasi-static compressive response of a porcine muscle. J Biomech 2007;40:2999–3005.
[6] Pervin F, Chen W. Dynamic mechanical response of bovine gray matter and white matter brain tissues under compression. J Biomech 2009;42:731–5.
[7] Cheng M, Chen W, Weerasooriya T. Mechanical behavior of bovine tendon with stress-softening and loading-rate effects. Adv Theor Appl Mech 2009;2(2):59–74.
[8] Edwards C, Marks R. Evaluation of biomechanical properties of human skin. Clin Dermatol 1995;13:375–80.
[9] Shergold OA, Fleck NA, Radford D. The uniaxial stress versus strain response of pig skin and silicone rubber at low and high strain rates. Int J Impact Eng 2006;32:1384–402.
[10] Birschoff JE, Arruda EM, Grosh K. Finite element modeling of human skin using an isotropic, nonlinear elastic constitutive model. J Biomech 2000;33: 645–52.
[11] Evans SL, Holt CA. Measuring the mechanical properties of human skin in vivo using digital image correlation and finite element modeling. J Strain Anal Eng 2009;44(5):337–45.
[12] Song B, Ge Y, Chen W, Weerasooriya T. Radial inertia effects in Kolsky bar testing of extra-soft specimens. Exp Mech 2007;47(5):659–70.
[13] Kolsky H. An investigation of the mechanical properties of materials at very high rates of loading. Proc Phys Soc B 1949;62:676–700.
[14] Gray G. Classic Split-Hopkinson pressure bar testing. In: Kuhn H, Medlin D, editors. ASM International, vol. 8; 2000. Material Park: OH, pp. 462-476.
[15] Gray G, Blumenthal W. Split-Hopkinson pressure bar testing of soft materials. In: Kuhn H, Medlin D, editors. ASM International, vol. 8; 2000. Material Park: OH, pp. 488–496.
[16] Nie X, Song B, Ge Y, Chen WW, Weerasooriya T. Dynamic tensile testing of soft materials. Exp Mech 2009;49:451–8.
[17] Frew DJ, Forrestal MJ, Chen W. Pulse shaping techniques for testing brittle materials with a split Hokinson pressure bar. Exp Mech 2002;42:93–106.
[18] Frew DJ, Forrestal MJ, Chen W. Pulse shaping techniques for testing elastic–plastic materials with a split Hokinson pressure bar. Exp Mech 2005;45:186–95.
[19] Chen W, Zhang B, Forrestal M. A split Hopkinson bar technique for low-impedance materials. Exp Mech 1998;39(2):81–5.
[20] Chen W, Lu F, Zhou B. A quartz-crystal-embedded split Hopkinson pressure bar for soft materials. Exp Mech 2000;40(1):1–6.
[21] Dunn MG, Silver FH, Swann DA. Mechanical analysis of hypertrophic scar tissue: structural basis for apparent increased rigidity. J Invest Dermatol 1985;84:9–13.
[22] Jansen LH, Rottier PB. Some mechanical properties of human abdominal skin measured on excised strips: a study of their dependence on age and how they are influenced by the presence of striae. Dermatologica 1958;117:65–183.
[23] Ogden RW. Large deformation isotropic elasticity – on the correlation of theory and experiment for incompressible rubberlike solids. P Roy Soc A – Math Phys 1972;326:565–84.
[24] Ogden RW, Saccomandi G, Sgura I. Fitting hyperelastic models to experimental data. Comput Mech 2004;34:484–502.